The disappearance of the re-entrant spin-glass state on annealing for the amorphous La - Fe alloy system

1996 J. Phys.: Condens. Matter 8 2053

(http://iopscience.iop.org/0953-8984/8/12/017)

J. Phys.: Condens. Matter **8** (1996) 2053–2062. Printed in the UK

The disappearance of the re-entrant spin-glass state on annealing for the amorphous La–Fe alloy system

S Terashima†, K Fukamichi†, H Aruga-Katori‡, T Goto‡, T H Chiang†, E Matsubara§ and Y Waseda‖

† Department of Materials Science, Faculty of Engineering, Tohoku University, Sendai 980-77, Japan

‡ Institute for Solid State Physics, The University of Tokyo, Roppongi, Minato-ku, Tokyo 106, Japan

§ Department of Metallurgy, Faculty of Engineering, Kyoto University, Kyoto 606, Japan

‖ Institute for Advanced Materials Processing, Tohoku University, Sendai 980, Japan

Received 28 March 1995, in final form 26 September 1995

Abstract. The effect of annealing on the magnetic phase diagram for the amorphous La–Fe alloy system has been investigated. The amorphous La–Fe alloys in the as-prepared state show re-entrant spin-glass behaviour, and the ferromagnetic region is extended by annealing. The Curie temperature and the magnetic moment per Fe atom are increased, and in contrast the spin freezing temperature and the high-field susceptibility are decreased by annealing. The re-entrant spin freezing temperature of the amorphous $La_{30}Fe_{70}$ alloy is not observed in the temperature range down to 2.5 K. The magnetization curves show relatively good saturation after annealing. The change in these magnetic properties on annealing is correlated with the structural change.

1. Introduction

Various amorphous Fe-based binary alloys have been investigated extensively (Moorjani and Coey 1984, Hansen 1991). The magnetic phase diagrams of amorphous M–Fe (M ≡ metal) alloys are classified into three types (Fukamichi *et al* 1989a, Wakabayashi *et al* 1990). The first group exhibits a direct transition from the paramagnetic to spin-glass state, and amorphous Y–Fe alloys prepared by sputtering belong to this group (Chappert *et al* 1981, Coey *et al* 1981, Fukamichi *et al* 1989a, b). The second group shows re-entrant spin-glass behaviour, that is the magnetic state changes from the paramagnetic to the ferromagnetic state and finally re-enters a spin-glass state with decreasing temperature. Several amorphous Fe-based alloy systems such as La–Fe, Ce–Fe and Lu–Fe belong to this group (Fukamichi *et al* 1989a, b). The third group exhibits re-entrant spin-glass behaviour in a limited concentration range, and ferromagnetic behaviour is observed in a wide range of compositions. Amorphous Zr–Fe alloys are reported to fall within this type (Hiroyoshi and Fukamichi 1981, 1982, Hiroyoshi *et al* 1983, Unruh and Chien 1983).

Since the magnetic properties are structure sensitive, various studies on the relation between the magnetic properties and the structural change have been carried out (Egami 1983, 1984). For instance, the Curie temperature of an amorphous $Zr_{19}Ta_7Fe_{74}$ alloy is decreased by annealing due to the structural relaxation (Prater and Merz 1981). In particular, the magnetic properties of amorphous Fe-based alloys would be drastically changed by annealing because the Fe–Fe interatomic distance (Matsuura *et al* 1988) is very close to

0953-8984/96/122053+10$19.50

the critical distance at which the ferromagnetic interaction with a large moment competes with the antiferromagnetic interaction with a small moment at around 2.5 Å (Wassermann 1990). Compared with other amorphous Fe-based alloys, amorphous Y–Fe alloys are quite unique because these alloys prepared by sputtering transform from the paramagnetic to the spin-glass state as mentioned before, but they exhibit re-entrant spin-glass behaviour in weak external magnetic fields (Fujita *et al* 1993) or on annealing (Suzuki *et al* 1994).

It has been reported that amorphous La_xFe_{100-x} alloys ($17.5 \leqslant x \leqslant 30.6$) are ferromagnetic because their magnetization curves show good saturation (Kazama *et al* 1979, 1980). However, re-entrant spin-glass behaviour has been confirmed in the concentration range $12.5 \leqslant x \leqslant 40$ (Wakabayashi *et al* 1990). Since the amorphous La–Fe alloy system has the lowest spin freezing temperature of various re-entrant-type amorphous Fe-based alloys (Fukamichi *et al* 1989a, b, Wakabayashi *et al* 1990), it is expected that re-entrant spin-glass behaviour in this system is suppressed by annealing.

In the present paper, the effect of annealing on the magnetic phase diagram of the amorphous La–Fe alloy system has been investigated. Furthermore, a structural analysis has been carried out by x-ray diffraction, and the change in the local atomic structure has been correlated with the disappearance of the re-entrant spin-glass state.

2. Experimental details

Amorphous La_xFe_{100-x} alloy samples ($x = 10$, 12.5, 15, 20, 25, 30, 33.3, 35 and 40) were prepared by high-rate DC sputtering on a water-cooled Cu substrate. Their thickness was about 0.2 mm after continuous sputtering for 3 d. The pressure of Ar gas and the target voltage during sputtering were 4×10^{-2} Torr and 1.0 kV, respectively. After sputtering, the Cu substrate was dissolved in a solvent, CrO_3 (500 g) + H_2SO_4 (27 cm^3) + H_2O (1000 cm^3), heated at 320 K. Annealing was carried out in a vacuum of 5×10^{-5} Torr at 473 K and 493 K for 0.5, 1, 2 and 3 h. The thermomagnetization and the magnetic cooling effect were measured with a SQUID magnometer. The AC magnetic susceptibility measurement from about 2.5 to 300 K was carried out by a mutual inductance method at 1 Oe and 80 Hz. Magnetization curves up to 390 kOe were measured using an induction method in a pulsed magnetic field (Yamada *et al* 1986). In order to calibrate the magnetization, measurements up to 55 kOe were also carried out with a SQUID magnetometer. The structural change caused by annealing was investigated by x-ray diffraction at room temperature. The room-temperature density was measured by the Archimedean method using toluene as a working fluid. The detailed procedures of structural analyses have been described elsewhere (Matsubara *et al* 1992, Chiang *et al* 1994).

3. Results and discussion

Figure 1 shows the annealing time dependence of the Curie temperature T_C for the amorphous $La_{33.3}Fe_{66.7}$ alloy. The full circles and the open circles denote the results for the alloys annealed at 473 K and 493 K, respectively. The triangle represents the result for the as-prepared alloy. The temperature T_C has been determined as the inflection point of the magnetization M versus temperature T curves measured in a low applied magnetic field such as 30 Oe. As shown in the figure, a marked increase in T_C occurs within about 0.5 h. Finally, the increase in T_C is saturated on annealing at 493 K for 2 h and at 473 K for 3 h. These results suggest that structural relaxation is substantially completed in these conditions. In the present paper, almost all samples have been annealed at 473 K for 3 h.

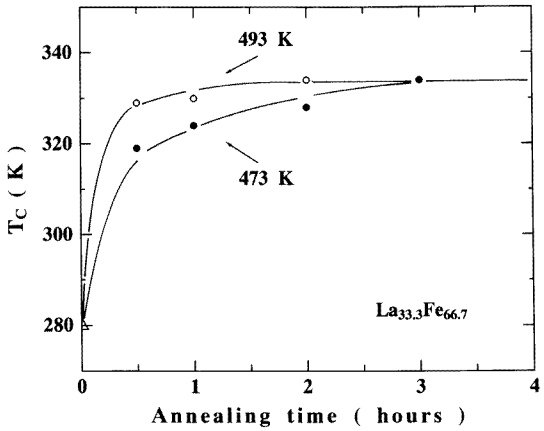

Figure 1. Annealing time dependence of the Curie temperature for the amorphous $La_{33.3}Fe_{66.7}$ alloy. The full circles and open circles denote the results for the alloys annealed at 473 K and 493 K, respectively. The triangle shows the result for the as-prepared alloy.

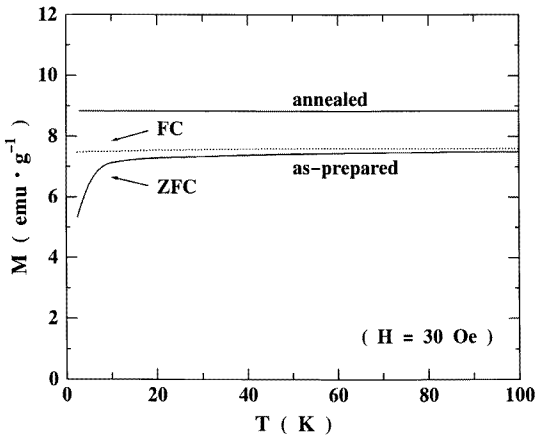

Figure 2. Temperature dependence of the ZFC and FC magnetizations measured at 30 Oe for the amorphous $La_{30}Fe_{70}$ alloys in the as-prepared state and in the annealed state at 473 K for 3 h.

The temperature dependences of the zero-field-cooled (ZFC) and field-cooled (FC) magnetization curves measured in 30 Oe for the amorphous $La_{30}Fe_{70}$ alloys in the as-prepared state and in the annealed state at 473 K for 3 h are shown in figure 2. As seen from the figure, the as-prepared sample exhibits a hysteresis between ZFC and FC magnetizations, being consistent with the previous results (Wakabayashi *et al* 1990). On the other hand, the annealed sample shows no hysteresis down to 2.5 K, indicating the disappearance of the spin-glass state in the measured temperature range. From these results, we can expect that annealing brings about the enlargement of the ferromagnetic region in the magnetic phase diagram in a similar manner to the amorphous Y–Fe alloys (Suzuki *et al* 1994).

Figure 3 shows the temperature dependence of magnetization M measured at 30 Oe

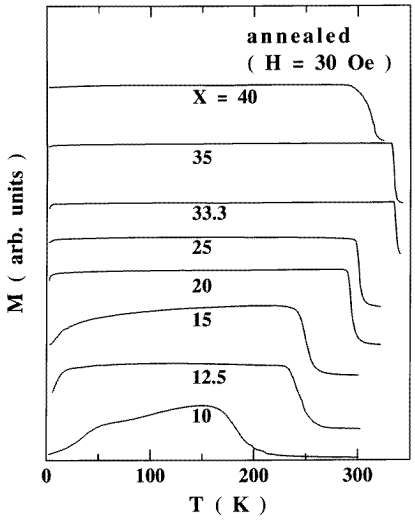

Figure 3. Temperature dependence of the magnetization measured at 30 Oe for the amorphous La_xFe_{100-x} alloys annealed at 473 K for 3 h.

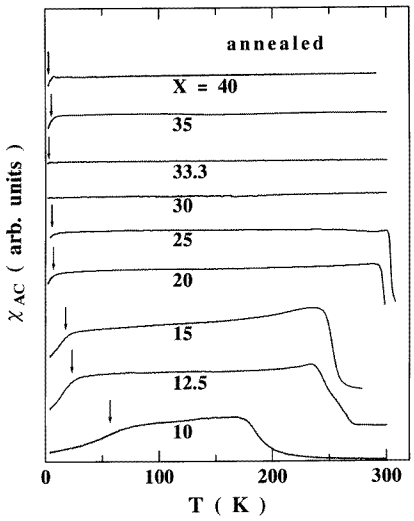

Figure 4. Temperature dependence of the AC magnetic susceptibility measured at 1 Oe and 80 Hz for the amorphous La_xFe_{100-x} alloys annealed at 473 K for 3 h. The arrows indicate the spin freezing temperature T_f.

for amorphous La_xFe_{100-x} alloys ($x = 10$, 12.5, 15, 20, 25, 33.3, 35 and 40) annealed at 473 K for 3 h. Almost all amorphous alloys show a decrease in M at low temperatures. Since the spin freezing temperature T_f is very sensitive to the applied magnetic field, the AC magnetic susceptibility χ_{AC} has been measured in a very low magnetic field of 1 Oe. Figure 4 shows the temperature dependence of χ_{AC} measured at 1 Oe and 80 Hz for the amorphous La_xFe_{100-x} alloys annealed at 473 K for 3 h. As seen from the figure, χ_{AC} decreases at low temperatures for all the measured samples except for $x = 30$. It should be noted that no decrease in χ_{AC} is observed down to 2.5 K for the annealed amorphous $La_{30}Fe_{70}$ alloy. Considering the results in figures 2–4, the annealed amorphous $La_{30}Fe_{70}$ alloy has no spin freezing temperature T_f down to 2.5 K, and other annealed amorphous La_xFe_{100-x} alloys ($x = 10$, 12.5, 15, 20, 25, 33.3, 35 and 40) are in the re-entrant spin-glass state. The arrows in this figure show T_f determined by the differential magnetic susceptibility measurement. No drastic variation in χ_{AC} with temperature around 300 K is observed above $x = 30$ because the Curie temperature is higher than room temperature as seen from figure 3. The flat temperature dependences of magnetization and susceptibility in figures 3 and 4 are mainly attributed to the demagnetization effect.

Figure 5 shows the magnetic phase diagram thus determined for the amorphous La–Fe alloy system annealed at 473 K for 3 h, together with that in the as-prepared state (Wakabayashi *et al* 1990). The full circles and open circles denote the results for the former and the latter, respectively. As shown in the figure, the ferromagnetic region becomes wider on annealing, i.e. T_C given by the solid line is increased and in contrast T_f by the broken line is decreased. It is worth noting that the amorphous $La_{30}Fe_{70}$ alloy has the highest T_C and the lowest T_f in the as-prepared state as seen from the figure. Consequently, no re-entrant spin-glass state is confirmed down to 2.5 K after annealing.

The magnetization curves up to 390 kOe measured at 4.2 K for the amorphous La_xFe_{100-x} alloys ($x = 10$, 15 and 20) annealed at 473 K for 3 h are shown in figure 6. The

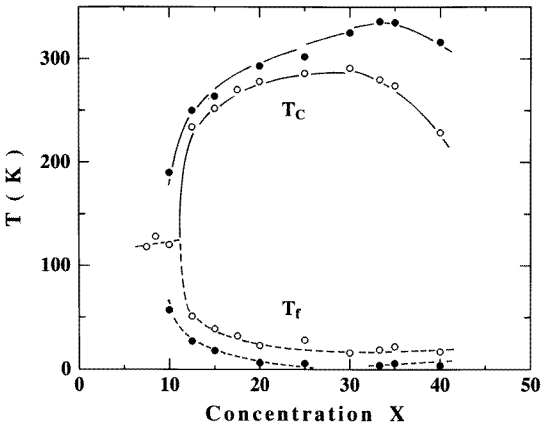

Figure 5. The magnetic phase diagram for the amorphous La–Fe alloy system. The open circles and full circles denote the results for the as-prepared samples (Wakabayashi *et al* 1990) and for the samples annealed at 473 K for 3 h, respectively. The Curie temperature T_C and the spin freezing temperature T_f are given by the solid line and broken line, respectively.

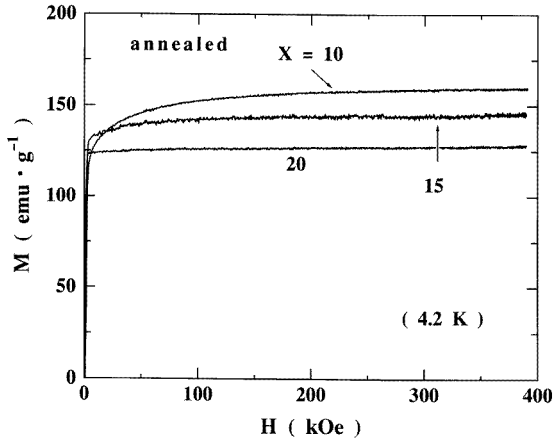

Figure 6. Magnetization curves up to 390 kOe measured at 4.2 K for the amorphous La_xFe_{100-x} alloys ($x = 10$, 15 and 20) annealed at 473 K for 3 h.

high-field susceptibility χ_{hf} and the magnetic moment μ_{Fe} per Fe atom have been obtained from the law of approach to saturation given by the following expression:

$$M = M_s\left(1 - \frac{a}{H^n} - \frac{b}{H^2}\right) + \chi_{hf}H \tag{1}$$

where M_s is the saturation magnetization, a and b are constants and H is the magntic field. In the present paper, the term b/H^2 is ignored in equation (1) because this term is related to magnetocrystalline anisotropy. The power n in the term a/H^n changes with respect to the origin of the deviation (Chudnovsky *et al* 1986). In the present paper, the magnetization curves for the annealed amorphous La–Fe alloys are well fitted by equation (1) with the power $n = 1$, although equation (1) with the power $n = 1/2$ is suitable for the magnetization curve for the as-prepared amorphous $La_{7.5}Fe_{92.5}$ alloy (Fujita *et al* 1995). Figures 7 and 8

show the concentration dependences of the high-field susceptibility χ_{hf} and the magnetic moment μ_{Fe} per Fe atom, respectively, for the amorphous La–Fe alloys annealed at 473 K for 3 h, together with those in the as-prepared state (Wakabayashi 1988, Wakabayashi *et al* 1990). In these figures, the full circles and open circles denote the results for the annealed alloys and the as-prepared alloys, respectively. As shown in figure 7, χ_{hf} of the former is lower than that of the latter because the magnetization curves show good saturation. On the other hand, μ_{Fe} is slightly increased by annealing as seen from figure 8.

Since the magnetic properties discussed above are correlated to the structural change induced by annealing, we have carried out a structural analysis. As shown in figure 1, an

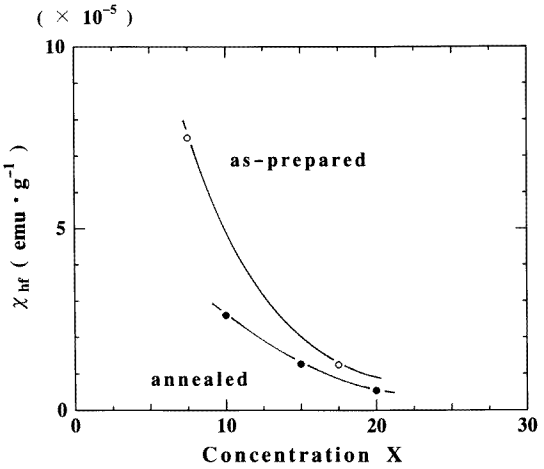

Figure 7. Concentration dependence of the high-field susceptibility χ_{hf} for the amorphous La–Fe alloy system. The open circles and full circles denote the results for the as-prepared samples (Wakabayashi 1988) and for the annealed samples at 473 K for 3 h, respectively.

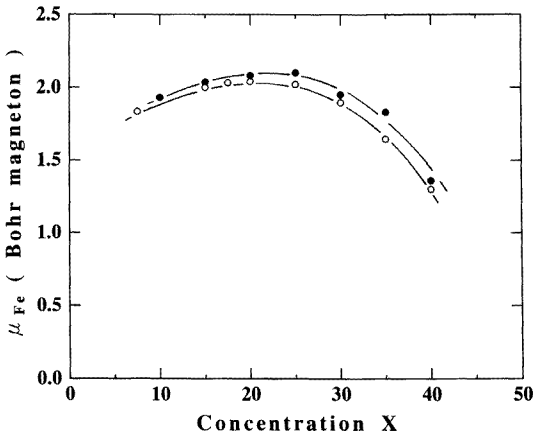

Figure 8. Concentration dependence of the magnetic moment μ_{Fe} per Fe atom for the amorphous La–Fe alloy system. The open circles and full circles denote the results for the as-prepared samples (Wakabayashi *et al* 1990) and for the annealed samples at 473 K for 3 h, respectively.

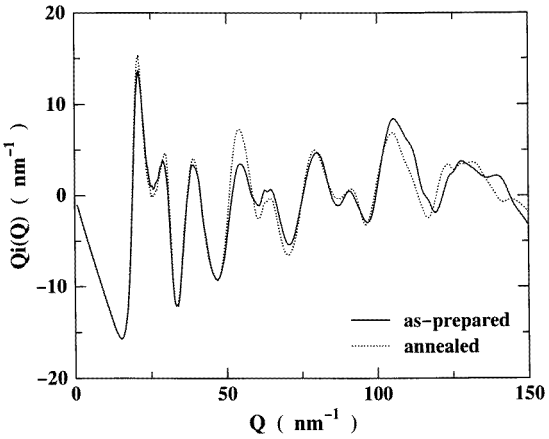

Figure 9. The interference functions of the amorphous $La_{33.3}Fe_{66.7}$ alloys. The solid line and dotted line denote the results for the as-prepared sample and for the annealed sample at 493 K for 0.5 h, respectively.

effective increase in the Curie temperature T_C is caused within about 0.5 h by annealing at 493 K, suggesting that the structural relaxation is substantially completed. Therefore, we have used the sample annealed at 493 K for 0.5 h. The x-ray scattering intensities were converted into absolute units per atom, $I_{eu}^{coh}(Q)$, by using the generalized Krogh–Moe–Norman method (Wagner *et al* 1965) with the x-ray atomic scattering factors including the anomalous dispersion correction (Ibers and Hamilton 1974) and the Compton scattering terms (Cromer 1969). Then, the interference functions $Qi(Q)$ for the present alloys are obtained from the following equation:

$$Qi(Q) = \left(I_{eu}^{coh}(Q) - \sum_{j=1}^{n} C_j f_j^2\right) \Big/ \left(\sum_{j=1}^{n} C_j f_j\right)^2 \tag{2}$$

where Q is given as $(4\pi \sin\theta)/\lambda$, λ is the wavelength, n is the total number of constituent elements, and C_j and f_j are the atomic fraction and the atomic scattering factor, respectively, of the element j. Figure 9 shows representative results on $Qi(Q)$ for the amorphous $La_{33.3}Fe_{66.7}$ alloys in the as-prepared state and in the annealed state at 493 K for 0.5 h. The solid line and dotted line denote the results for the former and the latter, respectively. The exact radial distribution function (RDF) in real space is given by the following expression (Warren 1969):

$$2\pi^2 r\rho(r) = 2\pi^2 r\rho_0 + \int_0^{Q_{max}} Qi(Q)\sin(Qr)\,\mathrm{d}Q \tag{3}$$

where $\rho(r)$ is the radial number density function and ρ_0 is the average number density of the sample. This RDF gives a better symmetrical shape for the peak than that of the conventional RDF, which has great merit for the peak-fitting process to determine the coordination and atomic distance. Figure 10 shows the RDF of the amorphous $La_{33.3}Fe_{66.7}$ alloys in the as-prepared state and the annealed state at 493 K for 0.5 h. The solid line and dotted line again denote the results for the former and the latter, respectively. Since the La atoms have no magnetic moment, we pay attention to the nearest-neighbour Fe–Fe pair whose distance is shown in figure 10. According to Mozzi–Warren (1969) method, the left-hand side of

equation (3) can be written as follows:

$$\sum_{j=1}^{n}\sum_{k=1}^{n}\frac{N_{jk}}{r_{jk}}\int_0^{Q_{max}}\frac{f_j f_k}{\langle f\rangle^2}\exp[-\alpha_{jk}^2 Q^2]\sin(Qr_{jk})\,\mathrm{d}Q = 2\pi^2 r\rho_0 + \int_0^{Q_{max}} Qi(Q)\sin(Qr)\,\mathrm{d}Q \tag{4}$$

where r_{jk} and N_{jk} are the interatomic distance and the coordination number of j–k pairs, respectively, f_j and f_k are the x-ray atomic scattering factors, $\langle f\rangle$ is the average atomic x-ray scattering factor and the term $\exp[-\alpha_{jk}^2 Q^2]$ is the convergence factor. In the present paper, the values of α for the as-prepared and annealed alloys are 0.021 and 0.016, respectively. By calculating the left-hand side of equation (4) after fitting the experimental RDF to the right-hand side, the interatomic distance r_{Fe-Fe} of the nearest-neighbour Fe–Fe pair, and the coordination number N_{Fe-Fe} of Fe atoms, respectively, have been obtained. The data on r_{Fe-Fe} and N_{Fe-Fe} for the amorphous $La_{33.3}Fe_{66.7}$ alloys in the as-prepared state and the annealed state at 493 K for 0.5 h are given in table 1. According to this table, there are overlapping errors in both r_{Fe-Fe} and N_{Fe-Fe}. However, the slight shift in the first peak for Fe–Fe pairs at about 0.250 nm is clearly seen in figure 10. This shift cannot be reversed even if the experimental error is taken into account. Therefore, the tendency of increase in the atomic distance for Fe–Fe pairs is clearly evident experimentally although the amount of the increase is small. Such a small change would result in a marked change in the magnetic properties because the magnetic properties of Fe are very sensitive to the atomic distance (Wassermann 1990). A similar result for an amorphous $Y_{20}Fe_{80}$ alloy has been reported (Suzuki *et al* 1995). It is interesting to note that this alloy exhibits a transition from the paramagnetic state to the spin-glass state which decreases in the as-prepared state, but it shows re-entrant spin–glass behaviour after annealing (Suzuki *et al* 1994).

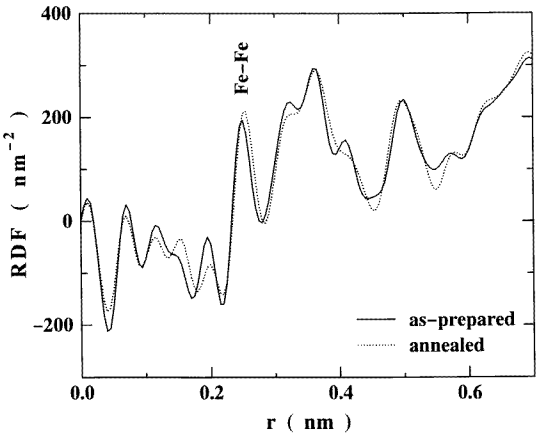

Figure 10. The exact RDFs of the amorphous $La_{33.3}Fe_{66.7}$ alloys. The solid line and dotted line denote the results for the as-prepared sample and for the annealed sample at 493 K for 0.5 h, respectively. The Fe–Fe indicates the distance of the nearest-neighbour Fe–Fe pair.

4. Conclusion

Amorphous La_xFe_{100-x} alloys prepared by high-rate DC sputtering were annealed, and the magnetic phase diagram has been investigated by AC and DC magnetic measurements. In

Table 1. The interatomic distance r_{Fe-Fe} and the coordination number N_{Fe-Fe} of the nearest-neighbour Fe–Fe pair for the amorphous $La_{33.3}Fe_{66.7}$ alloys in the as-prepared state and in the annealed state at 493 K for 0.5 h.

$La_{33.3}Fe_{66.7}$	r_{Fe-Fe} (nm)	N_{Fe-Fe}
As prepared	0.252 ± 0.002	6.0 ± 0.3
Annealed	0.254 ± 0.002	6.2 ± 0.3

the present paper, we have pointed out that there are three types of magnetic phase diagram for amorphous M–Fe (M ≡ metal) alloy systems. By annealing, however, the present amorphous La_xFe_{100-x} alloy system becomes ferromagnatic at $x = 30$. This implies that the three types of the magnetic phase diagram are not inherent in the Fe–based amorphous alloy systems. The main results are summarized as follows.

(1) The ferromagnetic state is enhanced by annealing, namely the Curie temperature is increased and the spin freezing temperature is decreased. In particular, the annealed amorphous $La_{30}Fe_{70}$ alloy has no spin freezing temperature down to 2.5 K.

(2) The magnetic moment is increased and the high-field susceptibility is decreased by annealing.

(3) The tendency of increase in the atomic distance on annealing is correlated with the change in the magnetic properties.

Acknowledgments

The authors wish to thank Dr Y Hattori and Mr A Fujita for valuable discussions. The research was supported by a Grant-in-Aid for Scientific Research (A) 04402045 from the Japanese Ministry of Education, Science and Culture.

References

Chappert J, Coey J M D, Liénard A and Rebauillat J P 1981 *J. Phys. F: Met. Phys.* **11** 2727–44

Chiang T H, Matsubara E, Kataoka N, Fukamichi K and Waseda Y 1994 *J. Phys.: Condens. Matter* **6** 3459–68

Chudnovsky E M, Saslow W M and Serota R A 1986 *Phys. Rev.* B **33** 251–61

Coey J M D, Givord D, Liénard A and Rebauillat J P 1981 *J. Phys. F: Met. Phys.* **11** 2707–25

Cromer D T 1969 *J. Chem. Phys.* **50** 4857–9

Egami T 1983 *Amorphous Metallic Alloys* ed F E Luborsky (London: Butterworth) pp 100–13

——1984 *Rep. Prog. Phys.* **47** 1601–725

Fujita A, Komatsu H, Fukamichi K and Goto T 1993 *J. Phys.: Condens. Matter* **5** 3003–10

Fujita A, Suzuki T, Terashima S, Fukamichi K, Aruga-Katori H and Goto T 1995 *Physica* B at press

Fukamichi K, Goto T, Komatsu H and Wakabayashi H 1989a *Proc. 4th Int. Conf. on the Physics of Magnetic Materials (Szczyrk-Bita, 1989)* ed W Gorkouski, H K Lachowicz and H Szymczak (Singapore: World Scientific) pp 354–81

Fukamichi K, Komatsu H, Goto T, Wakabayashi H and Matsuura M 1989b *Proc. MRS Int. Meeting on Advanced Materials (Tokyo, 1988) (Mater. Res. Soc. Symp. 11)* ed M Doyama (Pittsburg, PA: Materials Research Society) pp 285–99

Hansen P 1991 *Handbook of Magnetic Materials* vol 6, ed K H J Buschow (Amsterdam: North-Holland) pp 289–452

Hiroyoshi H and Fukamichi K 1981 *Phys. Lett.* **85A** 242–4

——1982 *J. Appl. Phys.* **53** 2226–8

Hiroyoshi H, Fukamichi K, Hoshi A and Nakagawa Y 1983 *High Field Magnetism* ed M Date (Amsterdam: North-Holland) pp 113–16

Ibers J A and Hamilton W C 1974 *International Tables for X-ray Crystallography* vol 4 (Birmingham: Kynoch) pp 148–51
Kazama N S, Fujimori H and Watanabe H 1979 *Sci. Rep. Res. Inst. Tohoku Univ.* A **27** 193–201
——1980 *J. Magn. Magn. Mater.* **15–8** 1423–4
Matsubara E, Waseda Y, Chiang T H and Fukamichi K 1992 *Mater. Trans. Japan Inst. Met.* **33** 155–7
Matsuura M, Fukunaga T, Fukamichi K and Suzuki K 1988 *Solid State Commun.* **66** 333–7
Moorjani K and Coey J M D 1984 *Magnetic Glasses* (Amsterdam: Elsevier) pp 339–52
Mozzi R L and Warren B E 1969 *J. Appl. Crystallogr.* **2** 164–72
Prater J T and Merz M D 1981 *J. Appl. Phys.* **52** 1877–9
Suzuki T, Fujita A, Fukamichi K, Aruga-Katori H and Goto T 1996 *J. Phys.: Condens. Matter* at press
Suzuki T, Fujita A, Fukamichi K and Goto T 1994 *J. Phys.: Condens. Matter* **6** 5741–50
Unruh K M and Chien C L 1983 *J. Magn. Magn. Mater.* **31–4** 1587–8
Wagner C N J, Ocken H and Joshi M L 1965 *Z. Naturforsch.* a **20** 325–35
Wakabayashi H 1988 *Doctoral Thesis* Tokyo Institute of Technology
Wakabayashi H, Goto T, Fukamichi K and Komatsu H 1990 *J. Phys.: Condens. Matter* **2** 417–29
Warren B E 1969 *X-ray Diffraction* (Reading, MA: Addison-Wesley) pp 135–42
Wassermann E F 1990 *Ferromagnetic Materials* vol 5, ed K H J Buschow and E P Wohlfarth (Amsterdam: North-Holland) pp 237–322
Yamada N, Takeyama S, Sakakibara T, Goto T and Miura N 1986 *Phys. Rev.* B **34** 4121–8